Mathematical Geology, Vol. 28, No. 7, 1996

Hierarchical Object-Based Stochastic Modeling of Fluvial Reservoirs[1]

Clayton V. Deutsch[2] and Libing Wang[2]

This paper describes a novel approach to modeling braided stream fluvial reservoirs. The approach is based on a hierarchical set of coordinate transformations involving relative stratigraphic coordinates, translations, rotations, and straightening functions. The emphasis is placed on geologically sound geometric concepts and realistically-attainable conditioning statistics including areal and vertical facies proportions. Modeling proceeds in a hierarchical fashion, that is (1) a stratigraphic coordinate system is established for each reservoir layer, (2) a number of channel complexes are positioned within each layer, and then (3) channels are positioned within each channel complex. The geometric specification of each sand-filled channel within the background of floodplain shales is a marked point process. Each channel is marked with a starting location, size parameters, and sinuosity parameters. We present the hierarchy of eight coordinate transformations, introduce an analytical expression for the channel cross-section shape, describe the simulation algorithm, and demonstrate how the realizations are made to honor local conditioning data from wells and global conditioning data such as areal and vertical proportions.

KEY WORDS: marked point processes, Boolean modeling, geostatistical reservoir modeling, coordinate transformation, data conditioning.

INTRODUCTION

Despite the fact that carbonate reservoirs host the majority of today's hydrocarbons, reservoirs of fluvial origin increasingly have become a major factor in newly proven reserves. A characteristic feature of many fluvial reservoirs is the presence of sinuous sand-filled channels within a background of floodplain shale. Techniques for realistically modeling the spatial distribution of channels are necessary for reliable volumetrics, connectivity assessment, and numerical input to flow simulation.

High-resolution sequence stratigraphy, made possible by dense 3D seismic and close-distance well-logging data, reveals a framework of the reservoir composed of repetitive strata bound by time-correlatable or chronostratigraphic sur-

[1] Received 15 January 1996; accepted 29 February 1996.

[2] Stanford Center for Reservoir Forecasting, Stanford University, Stanford, California 94305-2220; e-mail: clayton@pangea.stanford.edu and libing@pangea.stanford.edu

0882-8121/96/1000-0857$09.50/1

faces of erosion or nondeposition (van Wagoner and others, 1990). These strata may contain lithotypes that contrast drastically in petrophysical properties such as permeability and porosity. It is necessary to treat these surfaces as first-order heterogeneities for reservoir description and fluid-flow modeling. Once these strata are identified, the distribution of channel complexes vs. overbank deposits within each strata represents second-order heterogeneities. The distribution of individual channels within each channel complex constitutes third-order heterogeneities. Sequence stratigraphy allows such hierarchical classification of heterogeneities down to the bed set or bed level. This genetic hierarchy of heterogeneities within a given reservoir is best modeled through a hierarchical procedure.

Modeling proceeds sequentially. Each major stratigraphic layer is modeled independently one at a time. The channel complex distribution, within the layer-specific stratigraphic coordinate system, is established first. Then, within each channel complex, the distribution of individual channels is simulated within a transformed coordinate system. This process can be repeated down the hierarchy until the desired level of detail has been achieved. Finally, petrophysical properties such as porosity and permeability can be simulated with cell-based geostatistical algorithms and assigned to the corresponding facies.

This paper addresses the stochastic modeling of channel complexes and channels within a major reservoir layer. Multiple reservoir layers would be modeled successively and combined in a single reservoir model for volumetrics and flow simulation. At a higher level of iteration, multiple stochastic reservoir models could be constructed for assessing uncertainty.

An important feature of any approach to reservoir modeling is data conditioning. The data considered in this paper include lithofacies, porosity, and permeability data from wells, size and shape parameters of channel complexes, size and shape parameters of individual channels, vertical facies proportion curves, and areal facies proportion maps.

Our approach has been inspired by the clear geometries observed at outcrops and as viewed from airplane windows in modern fluvial settings. There are similar object-based approaches documented in the literature (Bridge and Leeder 1979; Clemensten and others, 1990; Hendriquez and others, 1990; Mackay and Bridge 1992, Tyler, Henriquez, and Svanes 1995). The approach adopted here is distinct from conventional object-based fluvial reservoir modeling in a number of ways: (1) an explicit reversable hierarchy of coordinate transformations that is keyed to sound sequence stratigraphic concepts; (2) geologically intuitive and accessible input data controlling channel sizes and shapes; (3) explicit control over vertically differing and really differing facies proportions; (4) realistic asymmetric channel geometries; (5) realistic nonundulating channel top surfaces; and (6) integrated porosity and permeability models where the main directions of continuity conform to channel geometries.

Table I. Summary of Eight-Step Coordinate Transformations from Largest to Smallest Scale

	Transform	Figure no.	From X	From Y	From Z	To X	To Y	To Z
1	Vertical Stratigraphic Coordinates	1	x_1	y_1	z_1	x_1	y_1	z_2
2	Areal Translation and Rotation	2	x_1	y_1	z_2	x_2	y_2	z_2
3	Channel Complex Translation and Rotation	3	x_2	y_2	z_2	x_3	y_3	z_2
4	Channel Complex Straightening	5	x_3	y_3	z_2	x_4	y_3	z_2
5	Relative Channel Complex Coordinate	6	x_4	y_3	z_2	x_5	y_3	z_2
6	Channel Translation	7	x_5	y_3	z_2	x_6	y_3	z_2
7	Channel Straightening	8	x_6	y_4	z_2	x_7	y_3	z_2
8	Relative Channel Coordinate	9	x_7	y_4	z_2	x_8	y_3	z_2

COORDINATE SYSTEMS

The key to the modeling approach presented in this paper is adapting the coordinate system to the appropriate principal directions of continuity. The direction of continuity depends on the scale of observation and the specific geological feature being modeled. Table 1 summarizes eight coordinate transformations from the largest scale to the smallest. Each step will be clarified next. Note the self similarity of coordinate transformations between channel complexes and individual channels. The initial reservoir coordinate system (x_1, y_1, z_1) may be any arbitrary system of two areal coordinates and an elevation coordinate (add a negative sign to positive depth coordinates).

No. 1: Vertical Transform to Stratigraphic Coordinates

Each major stratigraphic *layer* or *sequence* is modeled independently. The first step is to define a layer-specific relative stratigraphic coordinate from four structural grids: (1) the existing top z_{et}; (2) the existing base z_{eb}; (3) the restored top, z_{rt}; and (4) the restored base z_{rb}. As shown in Figure 1, the restored grids allow calculation of the stratigraphic coordinate as:

$$z_2 = \frac{z_1 - z_{rb}}{z_{rt} - z_{rb}} \quad (1)$$

where z_2 is the stratigraphic vertical coordinate and z_1 is the elevation of the data location. The coordinate z_2 is 0 at the stratigraphic (restored) based and 1 at the stratigraphic top and thus represents a relative time coordinate. Subsequent

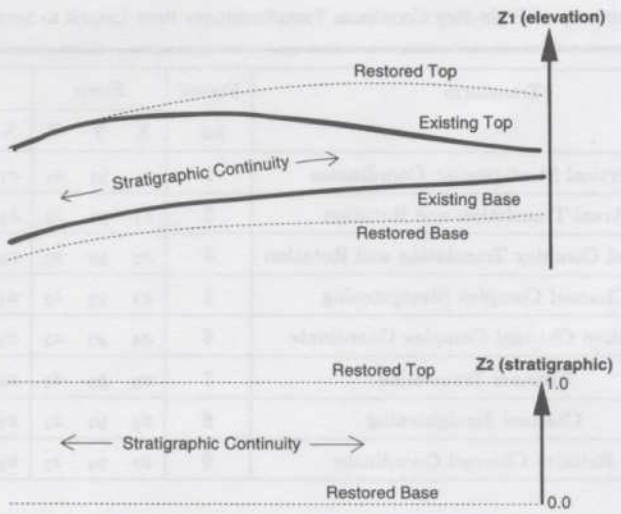

Figure 1. Coordinate transformation from original depth coordinate Z_1 to stratigraphic vertical coordinate Z_2.

modeling considers z_2 as the vertical coordinate. This transform may be reversed by:

$$z_1 = z_{rb} + z_2 \cdot (z_{rt} - z_{rb}) \tag{2}$$

Any backtransformed z_1 value outside of the interval $[z_{eb}, z_{et}]$ is not kept in the final model.

Faulted reservoirs must be "unfaulted" first by reversing the offset at each fault location. Left unchanged, faults may lead to the four grids being undefined at some locations and equivocally defined at other locations.

No. 2: Areal Translation and Rotation

The *reservoir* coordinate system is based on an arbitrary east x_1 and north y_1 coordinate system (perhaps UTM coordinates). An areal translation and rotation is carried out to obtain a coordinate system with a *stratigraphic* y_2 aligned with the principal paleoslope direction, that is, the direction that, on average, has the greatest continuity. The *stratigraphic* x_2 is perpendicular to y_2, and most often corresponds to the direction of least continuity.

Figure 2 illustrates the relationship between the two coordinate systems.

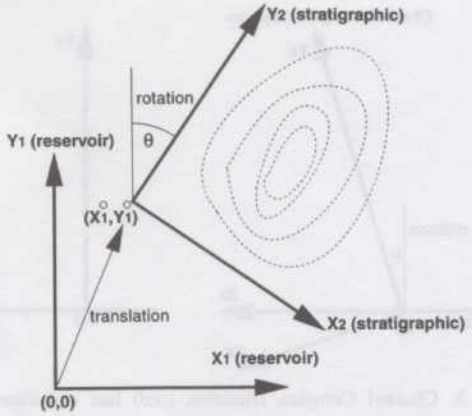

Figure 2. Areal transform (translation and rotation) from reservoir to stratigraphic coordinate systems.

Algebraically, they are related by the relations:

$$\begin{bmatrix} x_2 \\ y_2 \end{bmatrix} = \begin{bmatrix} \cos\theta & -\sin\theta \\ \sin\theta & \cos\theta \end{bmatrix} \begin{bmatrix} x_1 - x_1^0 \\ y_1 - y_1^0 \end{bmatrix} \tag{3}$$

and

$$\begin{bmatrix} x_1 \\ y_1 \end{bmatrix} = \begin{bmatrix} \cos\theta & \sin\theta \\ -\sin\theta & \cos\theta \end{bmatrix} \begin{bmatrix} x_2 \\ y_2 \end{bmatrix} + \begin{bmatrix} x_1^0 \\ y_1^0 \end{bmatrix} \tag{4}$$

where (x_1^0, y_1^0) is the location of the origin of the stratigraphic coordinate system is units of the reservoir/original coordinate system, and θ is the rotation angle defined clockwise from the north direction (y_1).

No. 3: Channel Complex Translation and Rotation

Fluvial channels may cluster together in *channel complexes*, also termed *channel belts*. A single large channel complex may be used to handle the situation where all individual channels are dispersed uniformly throughout the stratigraphic layer.

Figure 3 illustrates the channel complex direction (ccd) in the areal stratigraphic coordinate spce (x_2, y_2). A second areal translation and rotation is carried out to obtain a coordinate system with a ccd direction y_3 different from the predominant paleoslope direction (y_2) by an angle α, a direction x_3 perpendicular to ccd, and an origin at $(x_2^s, 0)$. The (x_2, y_2) and (x_3, y_3) coordinate systems are

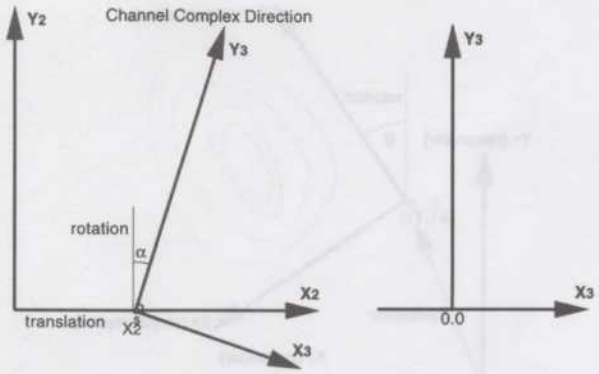

Figure 3. Channel Complex Direction (ccd) line and coordinate system.

related by relations:

$$\begin{bmatrix} x_3 \\ y_3 \end{bmatrix} = \begin{bmatrix} \cos\alpha & -\sin\alpha \\ \sin\alpha & \cos\alpha \end{bmatrix} \begin{bmatrix} x_2 - x_2^s \\ y_2 \end{bmatrix} \tag{5}$$

and

$$\begin{bmatrix} x_2 \\ y_2 \end{bmatrix} = \begin{bmatrix} \cos\alpha & \sin\alpha \\ -\sin\alpha & \cos\alpha \end{bmatrix} \begin{bmatrix} x_3 \\ y_3 \end{bmatrix} + \begin{bmatrix} x_2^s \\ 0 \end{bmatrix} \tag{6}$$

where α is the rotation angle defined clockwise from paleoslope direction y_2.

Corrected Width

For simplicity and consistency with previous coordinate systems, the width of a channel complex is measured perpendicular to y_3 coordinate direction. This causes the effective width of the channel complex to be too narrow when it is not aligned with the y_3 axis. The following correction is proposed to increase the apparent width $W_a(y)$ so that the effective width is constant:

$$W_a(y) = W(y)/\cos\beta(y) \tag{7}$$

where $\beta(y)$ is the angle between the y-coordinate and the local tangent to the channel center line. With $W_a(y)$, the construction of a channel reduces to setting a segment of length $W_a(y)$ centered at the channel line and perpendicular to the y-coordinate.

The effective width $W(y)$ of the channel complexes and channels are simulated. The apparent width $W_a(y)$ then is calculated. Note that $W_a(y)$ is defined

only for the interval $-90 < \beta < 90$. In other words, the channels are not allowed to roll over. This is not considered a limitation for braided stream environments. For meandering streams, however, a different approach would be required.

No. 4: Channel Complex Straightening

The center line of the channel complex undulates along the channel complex direction (ccd). Figure 4 shows the channel complex center line and the dashed lines that represent the channel areal limits. A piecewise linear function $f^{cc}(y_3)$ measures the deviation of the channel comlpex center line from the channel complex direction (ccd). A "straight" horizontal coordinate x_4 is defined then as the horizontal deviation from the channel complex center line:

$$x_4 = x_3 - f^{cc}(y_3) \tag{8}$$

This transform is reversed as:

$$x_3 = x_4 + f^{cc}(y_3)$$

The y and z coordinates are left unchanged.

No. 5: Relative Channel Complex Coordinate

The "straightened" channel complex is not equally wide along y_3. A relative horizontal coordinate x_5 is defined to make the channel complex boundaries parallel along y_3:

$$x_5 = \frac{2}{W_a(y_3)} \cdot x_4 \tag{9}$$

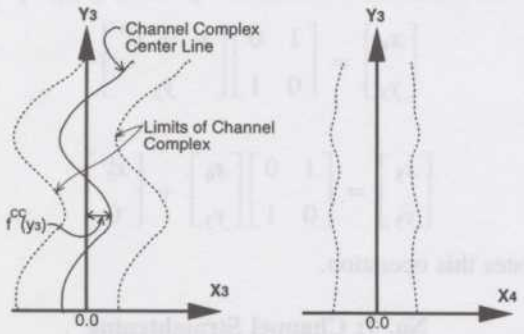

Figure 4. Transformation from channel complex direction to channel complex coordinates system following sinuous channel complex center line.

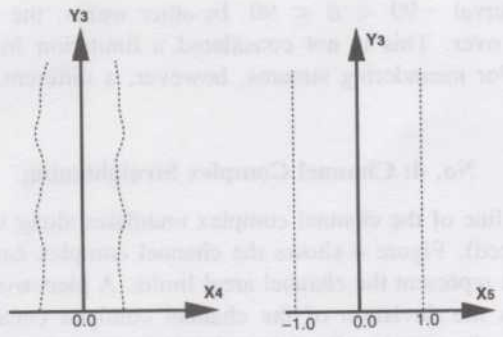

Figure 5. Transformation from channel complex coordinate system to relative channel complex coordinate system.

This transform is reversed as:

$$x_4 = \frac{W_a(y_3)}{2} \cdot x_5 \tag{10}$$

Once again, the y_3 and z coordinates are left unchanged. Figure 5 illustrates this operation.

No. 6: Channel Translation

This step involves the same operations as those utilized for the channel complex, that is translation and rotation, except that the rotation angle now is zero. A single translation is required to position a channel direction line within the channel complex. After that translation, the new coordinate system (x_6, y_3) is related to the old transformed coordinate system (x_5, y_3) by

$$\begin{bmatrix} x_6 \\ y_3 \end{bmatrix} = \begin{bmatrix} 1 & 0 \\ 0 & 1 \end{bmatrix} \begin{bmatrix} x_5 - x_5^{cs} \\ y_3 \end{bmatrix} \tag{11}$$

and

$$\begin{bmatrix} x_5 \\ y_3 \end{bmatrix} = \begin{bmatrix} 1 & 0 \\ 0 & 1 \end{bmatrix} \begin{bmatrix} x_6 \\ y_3 \end{bmatrix} + \begin{bmatrix} x_5^{cs} \\ 0 \end{bmatrix} \tag{12}$$

Figure 6 illustrates this operation.

No. 7: Channel Straightening

The center line of each channel undulates along the channel direction (see Fig. 7). A piecewise linear function $f^c(y_3)$ measures the deviation of the channel

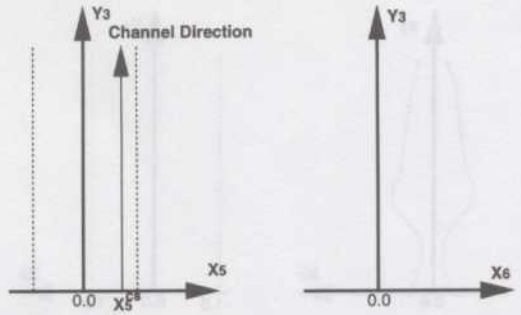

Figure 6. Individual channel direction coordinate system is obtained by translation from channel complex direction.

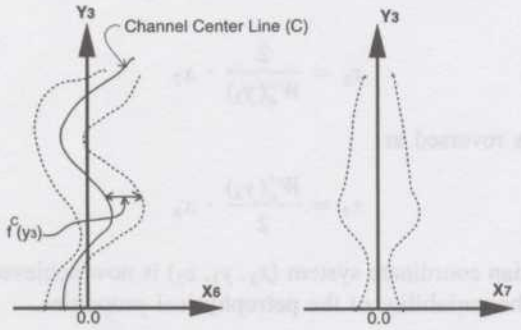

Figure 7. Transformation from channel direction to channel coordinate system following sinuous channel center line.

center line from the channel direction. A "straight" horizontal coordinate x_7 is defined as the horizontal deviation from the channel center line:

$$x_7 = x_6 - f^c(y_3) \tag{13}$$

This transform is reversed as:

$$x_6 = x_7 + f^c(y_3) \tag{14}$$

The y_3 and z coordinates are left unchanged.

No. 8: Relative Channel Coordinate

As was done for channel complex in No. 5, a relative horizontal coordinate x_8 is defined to make the channel boundaries parallel (see Fig. 8):

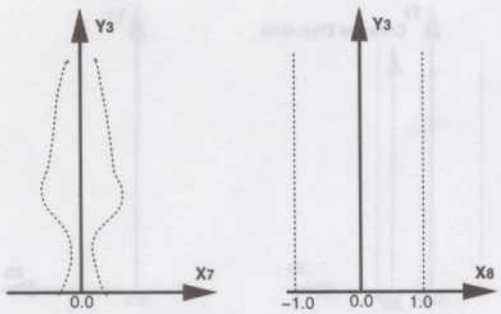

Figure 8. Transformation from channel coordinate system to relative channel coordinate system (between left bank and right bank) for modeling petrophysical properties such as porosity and permeability.

$$x_8 = \frac{2}{W_a^c(y_3)} \cdot x_7 \tag{15}$$

This transform is reversed as:

$$x_7 = \frac{W_a^c(y_3)}{2} \cdot x_8 \tag{16}$$

A regular Cartesian coordinate system (x_8, y_3, z_2) is now achieved within which one can model the variability of the petrophysical properties.

CHANNEL GEOMETRY AND CONSTRUCTION

The geometry of each channel is defined by a set of size parameters, location parameters, and 1D functions; namely, a center line coordinate, width, thickness, and the relative position of maximum thickness between the channel banks. The relative position of maximum thickness depends on the channel curvature (first subsection next). Analytical expressions for the position of maximum thickness and the channel cross-section geometry are presented in the second and third subsections next.

Channel Curvature

To define correctly the channel cross section the local curvature $C_r(y)$ of a channel center line is needed. As shown in Figure 9A, the curvature of a line $C_r(y)$ is calculated as:

$$C_r(y) = \frac{1}{\rho} = \lim_{\widehat{AB} \to 0} \frac{\theta}{\widehat{AB}} \tag{17}$$

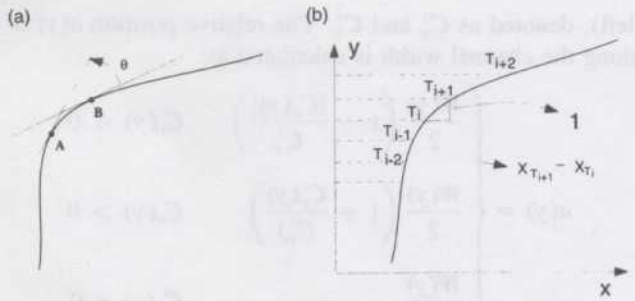

Figure 9. Curvature calculation along channel centerline.

where ρ is the radius of curvature, θ is the angle defined by the counterclockwise rotation going from the tangent at B to the tangent at A, and $\widehat{AB}$ is the length of arc AB.

The actual calculation of $C_v(y)$ in a discrete setting is illustrated in Figure 9B. The local curvature at node T_i can be calculated by the angle between tangents at T_i and T_{i+1} divided by the length of arc $T_i\hat{T}_{i+1}$ approximated by the following:

$$\widehat{T_iT_{i+1}} = \sqrt{1 + (x_{T_{i+1}} - x_{T_i})^2} \tag{18}$$

The angle between y-axis and tangent at node T_i can be approximated by:

$$\theta_{T_i} = \arctan(x_{T_{i+1}} - x_{T_i}) \tag{19}$$

Similarly, at node T_{i+1},

$$\theta_{T_{i+1}} = \arctan(x_{T_{i+2}} - x_{T_{i+1}}) \tag{20}$$

Then, the local curvature at node T_i is calculated as:

$$C_v(y_{T_i}) = \frac{\theta_{T_{i+1}} - \theta_{T_i}}{\widehat{T_iT_{i+1}}} \tag{21}$$

As described next, this curvature measure is used to help specify the channel cross-section.

Position of Maximum Thickness

The asymmetric channel cross-section is modeled with the position of maximum thickness closer to the outside bank of the channel. A deterministic positioning is proposed here; we could imagine a stochastic assignment with supporting outcrop data.

The first step is to scan through the entire centerline and calculate the local curvature $C_v(y)$. Denote the maximum absolute value of $C_v(y)$ of both signs

(right and left), denoted as C_v^r and C_v^l. The relative position $a(y)$ of maximum thickness along the channel width is calculated as:

$$a(y) = \begin{cases} \dfrac{W(y)}{2}\left(1 - \dfrac{|C_v(y)|}{C_v^l}\right) & C_v(y) < 0 \\ \dfrac{W(y)}{2}\left(1 + \dfrac{C_v(y)}{C_v^r}\right) & C_v(y) > 0 \\ \dfrac{W(y)}{2} & C_v(y) = 0 \end{cases} \tag{22}$$

Channel Cross-Section Geometry

Each sand-filled channel is defined geometrically by a channel width $W(y)$, maximum thickness $t(y)$, and the relative position $a(y)$ of the maximum thickness (see Fig. 10). The equation for the depth of the channel base below the channel top when $a(y) \leq 0.5$ (maximum thickness closer to the left bank) is:

$$d(w, y) = 4 \cdot t(y) \cdot \left(\frac{w}{W(y)}\right)^{b(y)} \cdot \left[1 - \left(\frac{w}{W(y)}\right)^{b(y)}\right] \tag{23}$$

where $b(y) = -Ln(2)/Ln(a(y))$, and $w \in [0, W(y)]$.

When $a(y) > 0.5$ (maximum thickness closer to the right bank as in Figure 10) the depth of the channel base below the channel top is given by:

$$d(w, y) = 4 \cdot t(y) \cdot \left(1 - \frac{w}{W(y)}\right)^{c(y)} \cdot \left[1 - \left(1 - \frac{w}{W(y)}\right)^{c(y)}\right] \tag{24}$$

where $c(y) = -Ln(2)/Ln(1 - a(y))$.

In the proposed simulation procedure, $W(y)$ is simulated and $a(y)$ is made a deterministic function of the local curvature of a simulated channel centerline. The function $d(w, y)$ defined by formulae (23) and (24) is symmetric at $a(y) = 0.5$.

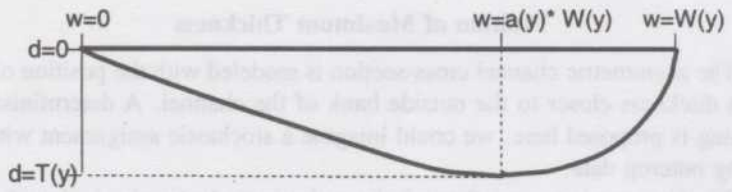

Figure 10. Vertical section of channel geometry.

The cross-section areal size at a given y coordinate, $S(y)$, may be used to calculate the volume of sand-filled channel:

$$S(y) = \int_{w=0}^{w=W(y)} d(w, y)dw$$

$$= \frac{4 \cdot t(y) \cdot W(y) \cdot k(y)}{2k^2(y) + 3k(y) + 1} \tag{25}$$

where

$$k(y) = \begin{cases} b(y) & \text{if } a(y) \leq .5 \\ c(y) & \text{if } a(y) > .5 \end{cases}$$

A 3D channel is constructed as a horizontally enlongated stack of 2D cross-sections along the y-coordinate direction. The shapes of these stacks along the y direction are determined by the parameters $W(y)$ and $a(y)$ simulated from smoothly varying stochastic fields. The volume of a channel, V, is the sum of the contributions of N such cross-sections: $V = \Sigma_{i=1}^{N} S(y_i)$.

Each channel is filled with porosity and permeability using the appropriate within-channel coordinate system. As shown in Figure 11, the vertical coordinate system could be parallel to the top channel surface or proportional between the top and base surfaces. Onlap correlation, where the correlation parallels the channel top, has been used in this paper. The base of each channel may have shale clasts or basal deposits that lower porosity and, more importantly, permeability. Furthermore, there may be a systematic trend in porosity from the base to the top of each channel. These features could be handled easily, because the

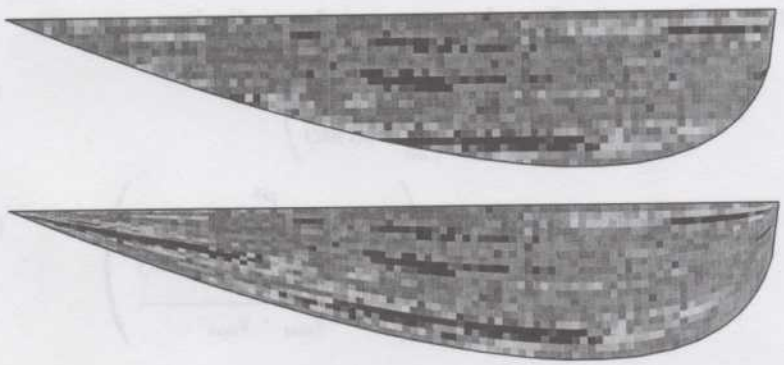

Figure 11. Vertical section of channel with two different vertical stratigraphic coordinates. Top channel illustrates an "onlap" correlation and lower channel illustrates "proportional" correlation; onlap correlation has been used in this paper.

position of each channel base is known, by a trend in the porosity modeling program.

GEOLOGICAL CONDITIONING DATA

The approach documented in this paper aims at simulating a distribution of channels within a reservior strata bound by chronostratigraphic surfaces. These surfaces are provided through well and seismic data, possibly with the aid of a mapping algorithm. Input data for the cell-based simulation of petrophysical properties can also be obtained from well and seismic data.

The geological and geometrical data inputs are discussed in this section. In practice, some data inputs will be difficult to infer from available well and seismic data. It then may be necessary to adapt measurements from analogue outcrops, modern depositional systems, and similar densely drilled fields.

Facies Proportions

The proportion of each facies type (channel sand, floodplain shale, crevasse splay sand, etc.) may be specified by a vertical proportion curve, an areal proportion map, and a reference global proportion. The reference global proportions are denoted by P_g^k, $k = 1, \ldots, K$ where K is the number of facies. A vertical proportion curve specifies the proportion of a facies k as a function of vertical elevation or time and is denoted as $P_v^k(z)$ where $z \in (0, 1]$. Areal proportion maps specify the facies proportion as a function of areal location (x, y) and are denoted as $P_a^k(x, y)$. These three types of proportions can be obtained through a combination of well and seismic data.

The vertical proportion curve and areal proportion map have implicit global proportions that may be inconsistent either with each other or the reference global proportion; therefore, they are rescaled accordingly:

$$P_v^k(z) = P_v^k(z) \cdot \left(\frac{P_g^k}{\int_0^1 P_v^k(z)dz} \right) \tag{26}$$

$$P_a^k(x, y) = P_a^k(x, y) \cdot \left(\frac{P_g^k}{\dfrac{\int_0^{x_{max}} \int_0^{y_{max}} P_a^k(x, y)dxdy}{x_{max} \cdot y_{max}}} \right) \tag{27}$$

Channel Complex and Channel Geometry

A collection of closely spaced and genetically related channels is referred to as a channel complex. As described, the orientation, shape, and size of a

channel complex serve as a basic modeling unit. The following input distributions are required to specify the channel complex geometry: (1) angles α (see Fig. 3); (2) departure from channel complex direction $f^{cc}(y_3)$ (see Fig. 4) and correlation length in the y_3 direction; (3) thickness; (4) width-to-thickness ratio; and (5) net-to-gross ratio within the channel complex.

A greater number of parameters are required to specify the channel geometry because the thickness and width of each channel is not constant: (1) departure from channel complex direction $f^{c}(y_3)$ (see Fig. 7) and correlation length in the y_3 direction; (2) average thickness; (3) thickness undulation and correlation length of thickness undulation; (4) width-to-thickness ratio; (5) width undulation and correlation length of width undulation; and (6) channel base roughness.

Two characteristics of the geological/geometrical parameters required for modeling are that (1) each parameter may take a range of possible values according to a probability distribution, and (2) the range of values changes with the stratigraphic position/time z. Therefore, the following geological inputs will be specified with a series of conditional distributions for a discrete set of z values between the stratigraphic base ($z = 0$) and the stratigraphic top ($z = 1$), for example, $F(g|(z))$ for the cdf of parameter g given stratigraphic position z. Figure 12 illustrates how the quantile values could change with time or z level.

For simplicity, all distributions are specified by a series of quantile values. When required, linear interpolation is used between known quantiles and the distributions will be assumed to follow multivariate Gaussian distributions after normal-score transformation (see Deutsch and Journel, 1992, p. 211) are modeled to honor fine-scale porosity and permeability variations.

Well Data

The facies, porosity, and permeability values are known along each well; noncored wells may have only facies and porosity data. At some fine level of resolution (say, each decimeter along a well) the well data may be recorded at each of n intervals as $f(\mathbf{u}_i)$, $\phi(\mathbf{u}_i)$, $k(\mathbf{u}_i)$, $i = 1, \ldots, n$ where f is a categorical variable giving the facies, ϕ is the porosity expressed as a fraction, k is the permeability in milliDarcies, the n data may come from any arbitrary number of wells, and the location vectors $\mathbf{u}_i$, $i = 1, \ldots, n$ may be set arbitrarily to the x_2, y_2, z_2 coordinate system for modeling a specific reservoir layer. Recall that all coordinate conversions are reversible; therefore, knowing the locations of the well data in one set of coordinates provides nonequivocal knowledge in all coordinate systems.

SIMULATION PROCEDURE

Each reservoir layer is modeled independently and then merged with other layers according to appropriate erosion and truncation rules. For a given layer,

all data are converted to the x_2, y_2, z_2 coordinate system (see Table 1). All of the geologic inputs described must be specified prior to modeling. We expect that many of these parameters will be difficult to infer from available data. Some parameters, such as width-to-thickness ratios, may be kept constant at some realistic value, say 50:1 (real distance units). Sensitivity studies can be considered on other parameters to judge the importance and to assess the visual acceptability of the resulting realizations.

The simulation procedure is sequential. First, the channel complex distribution is established. Second, the distribution of channels within each channel complex. Third, the porosity is assigned using appropriate channel coordinates. Finally, the permeability is assigned conditional to the facies and porosity. Only the first two steps will be described here because conventional algorithms can be used for porosity and permeability modeling.

Conditioning to the facies succession along wells and to facies proportion data is accomplished via an objective function that measures mismatch from the known facies at wells and proportion curves and maps. At each stage of simulation an iterative procedure is used to perturb the set of channel complexes or channels until an acceptably low objective function is obtained.

For notation, the * is used to identify quantities from a stochastic realization and the absence of a * will identify reference or target quantities, for example, $P_v^k(z)$ is the reference proportion of facies k at level z and $P_v^{k*}(z)$ is the actual proportion of facies k at level z in a realization.

Channel Complex Simulation

Each channel complex is a volume within which a number of channels ultimately will be placed. The indicator variable

$$i_{cc}(\mathbf{u}) = \begin{cases} 1 & \text{if } \mathbf{u} \text{ is within a channel complex} \\ 0 & \text{otherwise} \end{cases}$$

defines whether a channel complex is present or absent at any location $\mathbf{u}$. Knowing the number of channel complexes and their geometric parameters it is possible to define $i_{cc}(\mathbf{u})$ for all locations in the area of interest. The presence of a channel complex does not imply necessarily the presence of a channel. Each channel complex has a net-to-gross ratio (proportion of channel facies) less than 1.0. The proportion of channel facies at each location, $p_{cc}(\mathbf{u})$, is zero outside of a channel complex and defined from the channel complex net-to-gross ratio when in a channel complex. When two channel complexes overlap at location $\mathbf{u}$ the one with the higher stratigraphic position z takes precedence.

The distribution of channel complexes should honor well data and coarse-scale facies proportions. At this coarse scale, there are two constraints as a result

of well data: (1) a channel complex must be present where a channel is intersected by a well, and (2) a channel complex should not be present at long (defined by the size of the channel complexes) intersections of nonchannel facies. To quantify the first constraint another indicator variable is defined for all well intersections:

$$i_w(\mathbf{u}_i) = \begin{cases} 1 & \text{if } \mathbf{u}_i \text{ is within a channel} \\ 0 & \text{otherwise} \end{cases} \qquad i = 1, \ldots, n$$

A second well-based indicator variable will be defined to flag those locations that are surely outside of a channel complex:

$$j_w(\mathbf{u}_i) = \begin{cases} 1 & \text{if } \mathbf{u}_i \text{ is within distance } d_{\max} \text{ of a location} \\ & \mathbf{u}_l,\ l = 1, \ldots, n \text{ where } i_w(\mathbf{u}_l) = 1 \qquad i = 1, \ldots, n \\ 0 & \text{otherwise} \end{cases}$$

The magnitude of the distance $d_{\max}$ is on the order of the size of a channel complex, for example, it could be set to the average channel complex size.

Now, the objective function for channel complex simulation could contain five components relating to facies proportions and well data:

$$\begin{aligned} O_{CC} = {} & \omega_1 \cdot \sum_{k=1}^{K} [P_g^k - P_g^{k*}]^2 + \omega_2 \cdot \sum_{k=1}^{K} \sum_{z=1}^{N_z} [P_v^k(z) - P_v^{k*}(z)]^2 \\ & + \omega_3 \cdot \sum_{k=1}^{K} \sum_{x=1}^{N_x} \sum_{y=1}^{N_y} [P_a^k(x, y) - P_a^{k*}(x, y)]^2 \\ & + \omega_4 \cdot \sum_{i:i_w(\mathbf{u}_i)=1} [i_w(\mathbf{u}_i) - i_{cc}(\mathbf{u}_i)]^2 \\ & + \omega_5 \cdot \sum_{i:j_w(\mathbf{u}_i)=0} [j_w(\mathbf{u}_i) - i_{cc}(\mathbf{u}_i)]^2 \end{aligned} \tag{28}$$

where ω_i is a weight to objective function component i. These weights are determined automatically such that each component has equal importance approximately (see Deutsch and Cockerham, 1994). Estimates of the proportions P_g^{k*}, $P_v^{k*}(z)$, and $P_a^{k*}(x, y)$ are calculated from $p_{cc}(\mathbf{u})$.

The goal at this stage of simulation is to establish the K channel complexes and their geometric attributes. This is done in an iterative fashion:

(1) Start with no channel complex: $K = 0$, that is empty arrays $i_{cc}(\mathbf{u}) = 0$, $\forall \mathbf{u} \in A$, and $p_{cc}(\mathbf{u}) = 0.0$, $\forall \mathbf{u} \in A$.

(2) Define an array of operations: *add*, *remove*, *translate*, and *rotate*. Randomly select one operation from this array and perform the operation. Initially, channel complexes will be added.

(3) Update the objective function O_{CC} and decide the acceptance or rejection of that operation according to the decision rule [could use a simulated annealing schedule or some other scheme (Deutsch and Cockerham, 1994)]. If needed, update the list of channel complexes, the $i_{cc}(\mathbf{u})$ variable, and the $p_{cc}(\mathbf{u})$ variable.

(4) Return to step 2 until O_{CC} is deemed low enough.

The parameters for each of the operations *add*, *remove*, and *rotate* drawn from the geological/geometrical input distributions; therefore, the size and shape distributions are honored in the final realization.

When the simulation is finished the computer program can report the list of channel complexes and their parameters, a raster image of the $i_{cc}(\mathbf{u})$ and $p_{cc}(\mathbf{u})$ variables, and summaries of data conditioning.

Channel Simulation

The goal now is to specify the channel distribution within the channel complexes. A new indicator variable

$$i_c(\mathbf{u}) = \begin{cases} 1 & \text{if } \mathbf{u} \text{ is within a channel} \\ 0 & \text{otherwise} \end{cases}$$

defines whether a channel is present or absent at any location **u.** This indicator variable can be retrieved everywhere in the model by the geometric description of all channels.

The distribution of channels should honor well data and facies proportions. At this final finer scale, there is a single constraint because of well data: a channel must be present where a channel is intersected by a well and a channel should not be present where a channel is not intersected by a well. The $i_w(\mathbf{u}_i)$, $i = 1, \ldots, n$ indicator variable as defined will be considered.

Now, the objective function for channel simulation could contain four components relating to facies proportions and well data:

$$\begin{aligned} O_C = {} & \omega_1 \cdot \sum_{k=1}^{K} [P_g^k - P_g^{k*}]^2 + \omega_2 \cdot \sum_{k=1}^{K} \sum_{z=1}^{N_z} [P_v^k(z) - P_v^{k*}(z)]^2 \\ & + \omega_3 \cdot \sum_{k=1}^{K} \sum_{x=1}^{N_x} \sum_{y=1}^{N_y} [P_a^k(x, y) - P_a^{k*}(x, y)]^2 \\ & + \omega_4 \cdot \sum_{i=1}^{n} [i_w(\mathbf{u}_i) - i_c(\mathbf{u}_i)]^2 \end{aligned} \tag{29}$$

where ω_i is the weight applied to objective function component i. These weights are determined automatically such that each component has equal importance

approximately (see Deutsch and Cockerham, 1994). Estimates of the proportions P_g^{k*}, $P_v^{k*}(z)$, and $P_a^{k*}(x, y)$ are calculated from the channel indicator variable $i_c(\mathbf{u})$.

At this stage of simulation the goal is to establish the number L_k, $k = 1, \ldots, K$ of channels within each channel complex and their geometric attributes. This is done in an iterative fashion:

(1) Start with no channel: $L_k = 0$, $k = 1, \ldots, K$, that is, an empty array $i_c(\mathbf{u}) = 0$, $\forall\ \mathbf{u} \in A$.
(2) Define an array of operations: *add*, *remove*, *translate*, and *rotate*. Randomly select one operation from this array and perform the operation. Initially, channels will be added.
(3) Update the objective function O_C and decide the acceptance or rejection of that operation according to the decision rule [a simulated annealing schedule or some other scheme (Deutsch and Cockerham, 1994) could be used)]. If needed, update the list of channels and the $i_c(\mathbf{u})$ variable.
(4) Return to step 2 until O_C is deemed low enough.

The parameters for each of the operations *add*, *remove*, and *rotate* are drawn from the geological/geometrical input distributions; therefore, the size and shape distributions are honored in the final realization.

When the simulation is finished the computer program can report the list of channels and their parameters, a raster image of the $i_c(\mathbf{u})$ and summaries of data conditioning.

Porosity/Permeability Simulation

The porosity and permeability within each channel is simulated independently using conventional geostatistical algorithms such as sequential Gaussian simulation, indicator simulation, or annealing-based algorithms (Deutsch and Journel, 1992). The well data ($\phi(\mathbf{u}_i)$, $k(\mathbf{u}_i)$, $i = 1, \ldots, n$), transformed to the appropriate x_8, y_3, z_2 coordinate system, are used as conditioning data when they fall within the boundaries of the channel.

EXAMPLES

The simulation algorithm described here was coded in both C and FORTRAN. Figure 12 shows isometric views of a channel complex distribution, a channel distribution, and a porosity distribution. This $100 \times 100 \times 50$ (500,000 cell) realization was constrained only to input distributions of geometric parameters and a global net-to-gross ratio of 0.50. There were 13 channel complexes containing 123 channels.

Figure 13 shows representative cross-sections through models that were

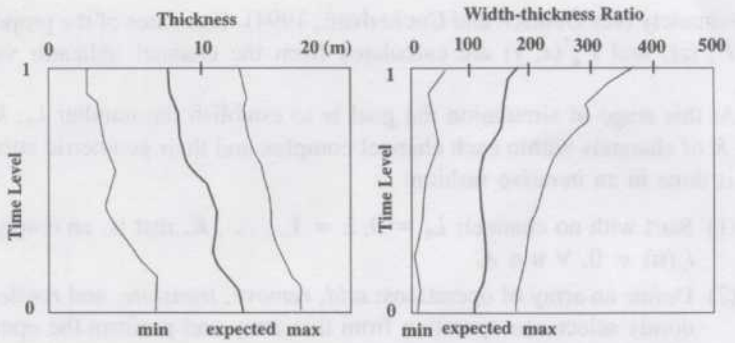

Figure 12. Charts illustrating distributions of channel thickness and width-thickness ratio as function of time level.

constructed to honor two different proportion curves. In both examples, the models reasonably reproduce the proportion curve. Note that the lower example (highest net-to-gross ratio near the center of the layer) matches the target proportions better because the channels are smaller. Figure 14 shows the result of conditioning to an areal proportion map. In this situation, the areal proportion

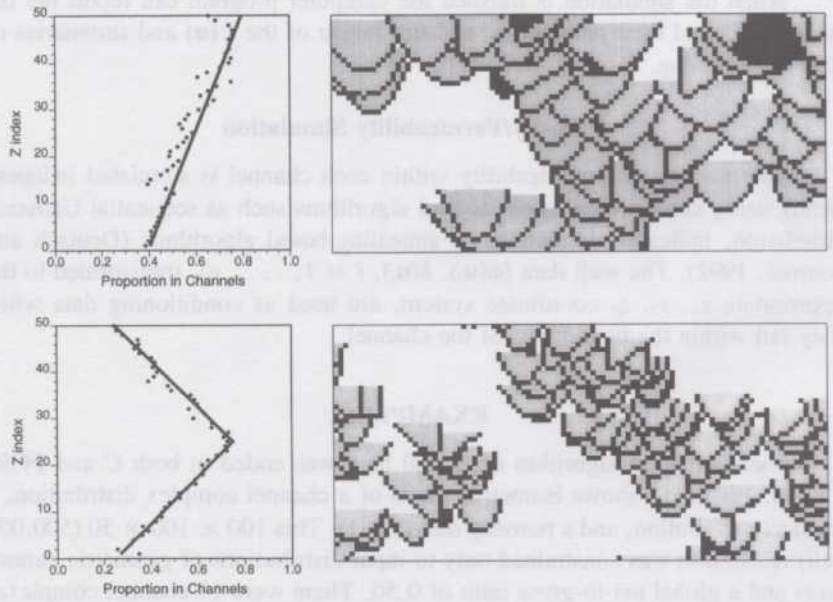

Figure 13. Target vertical proportion curve (solid line), experimental result (black dots), and example section through two different models.

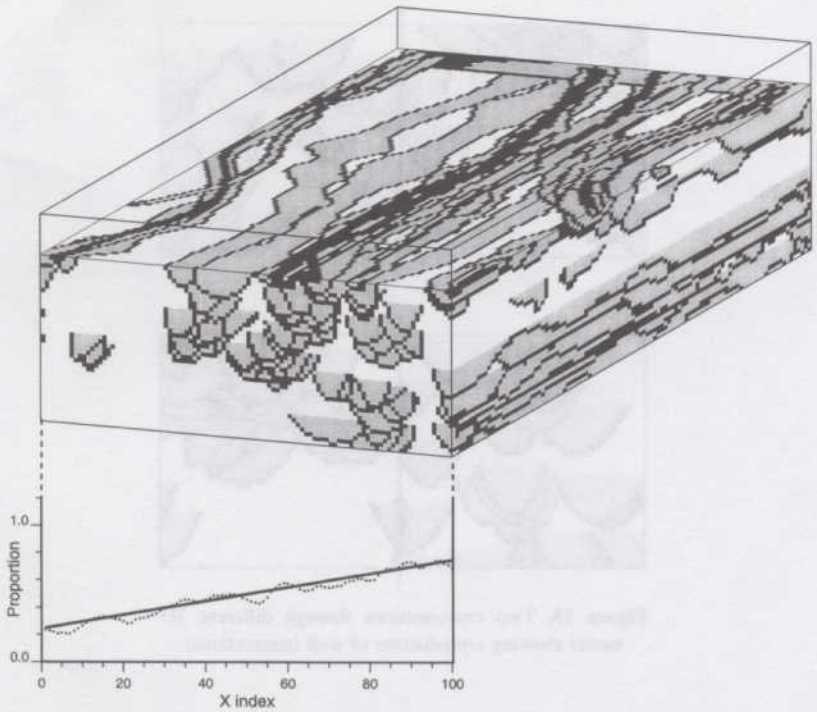

Figure 14. Target areal proportion (same for all y) shown as solid line on proportion profile. Black dots black dots show results of realization illustrated in block diagram.

increases to the east from 0.25 to 0.75. The profile on the bottom of Figure 14 shows the excellent reproduction of the map.

Figure 15 shows two representative cross-sections through models constructed to honor channel intersections at a well location. The channels do not match exactly at the top and base of the channel intersections. They could be made to match closer by running the iterative procedure longer or post-processing the realization and adjusting specific channels up or down. Note also that it would be possible to honor sand-on-sand channel boundaries through an additional component in the objective function.

The CPU time increases when data conditioning constraints are added. To generate the channel distribution for this 500000 cell example, on a Silicon Graphics POWER Indigo 2, it took 69 sec to generate an unconditional distribution, 230 sec when honoring vertical proportion curves, 264 sec when honoring the areal proportion map, and 305 sec to honor well data. Adding multiple constraints to the objective function does not significantly decrease the CPU

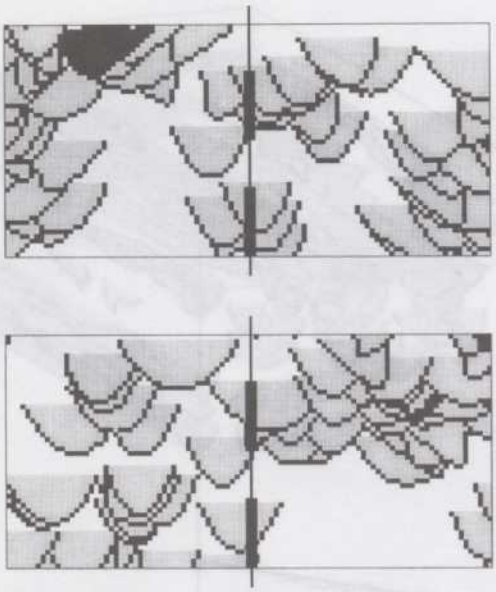

Figure 15. Two cross-sections through different 3D model showing reproduction of well intersections.

speed. For example, considering a vertical proportion curve and the well data took 279 sec (less than well data alone). Assigning porosity to the 123 channels in the unconditional realization took 579 sec using a sequential Gaussian simulation program, SGSIM (Deutsch and Journel, 1992); see Figure 16.

CONCLUSIONS

One conclusion of this paper is that reservoir modeling should proceed in a hierarchical or sequential scheme: (1) independently build multiple equiproable stochastic reservoir models; (2) independently model each major reservoir layer bounded by chronostratigraphic surfaces; (3) model the distribution of channel complexes to honor well data and perhaps locally differing proportions; (4) position channels within each channel complex to honor well data and a more detailed representation of the facies proportions; and then (5) assign porosity and permeability in a coordinate system aligned with the channel coordinates. This can be seen as a hybrid combination of object-based modeling for major geological features and cell-based modeling for porosity and permeability.

An eightfold set of coordinate transformations makes it possible to model geometrically complex fluvial reservoir features. Because each transform is re-

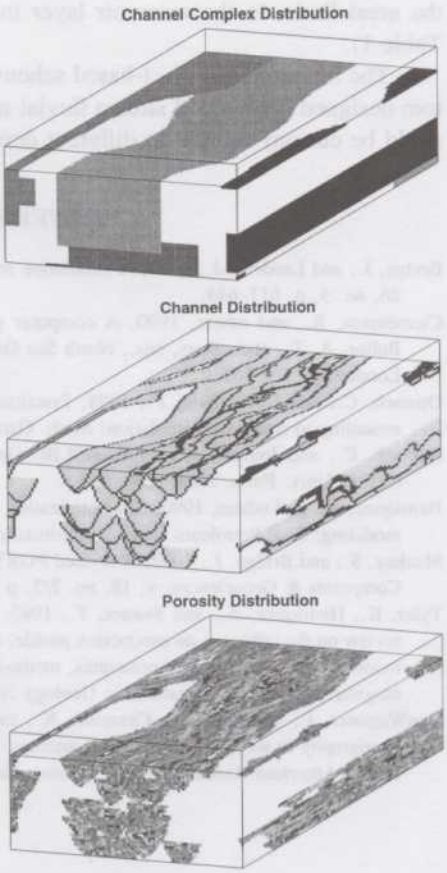

Figure 16. Example of channel complex, channel, and porosity distribution. Channel complexes are shaded according to average net-to-gross (medium stipple is close to 1.0 and dark-gray stipple 0.9). Bottom cell of every channel has been gray stipple to help identify channels and to show erosion rules. Porosity has been coded with light stipple being low porosity and dark stipple high porosity.

versible, it is straightforward to reconstruct the model in any coordinate system and to accomplish data conditioning at any level of coordinate transformation. In practice, the distributions of geometric/geologic parameters may be difficult to infer from available reservoir data. It will be necessary to borrow such distributions from outcrops, modern analogs, and densely drilled fields. The geologic input parameters required by this modeling approach are consistent with modern sequence stratigraphic concepts.

The iterative approach to honoring local conditioning data and vertical or areal average facies proportions is computationally efficient. This efficiency is the result of the sequential nature of conditoning; the channel complexes are positioned to honor coarse-scale features, channels then are positioned to honor fine-scale facies data, but porosity, and permeability where x_{max} and y_{max} are

the areal limits to the reservoir layer in the x_2 and y_2 coordinate system (see Table 1).

The hierarchical object-based scheme presented in this paper has been custom designed for braided stream fluvial reservoirs. Similar hierarchical schemes could be custom-tailored to different depositional environments.

REFERENCES

Bridge, J., and Leeder, M., 1979, A simulation model of alluvial stratigraphy: Sedimentology, v. 26, no. 5, p. 617–644.

Clemensten, R., and others, 1990, A computer program for evaluation of fluvial reservoirs, *in* Buller, A. T., and others, eds., North Sea Oil and Gas Reservoirs II: Graham and Trotman, London, p. 373–385.

Deutsch, C., and Cockerham, P., 1994, Practical considerations in the application of simulated annealing to stochastic simulation: Math. Geology, v. 26, no. 1, p. 67–82.

Deutsch, C., and Journel, A., 1992, GSLIB: Geostatistical Software Library and user's guide: Oxford Univ. Press, New York, 340 p.

Henriquez, A., and others, 1990, Characterization of fluvial sedimentology for reservoir simulation modeling: Soc. Petroleum Engineers Formation Evaluation Jour., v. 5, no. 3, p. 211–216.

Mackey, S., and Bridge, J., 1992, A revised FORTRAN program to simulate alluvial stratigraphy. Computers & Geosciences, v. 18, no. 2/3, p. 119–181.

Tyler, K., Henriquez, A., and Svanes, T., 1995, Modeling heterogeneities in fluvial domains: a review on the influence on production profile, *in* Yarus, J., and Chambers, R., eds., Stochastic modeling and geostatistics: principles, methods, and case studies: Am. Assoc. Petroleum Geologists Computer Applications in Geology No. 3, p. 77–89.

VanWagoner, J., Mitchum, R., Campion, K., and Rahmanian, V., 1990, Siliciclastic sequence stratigraphy in well logs, cores, and outcrops: Concepts for high-resolution correlation of time facies: American Association of Petroleum Geologists, Tulsa, Oklahoma, 55 p.